International Journal of Electrical, Electronic and Communication Sciences
ISSN: 2517-9438
Vol:10, No:3, 2016

# Selection of Wind Farms to Add Virtual Inertia Control to Assist the Power System Frequency Regulation

W. Du, X. Wang, Jun Cao, H. F. Wang

***Abstract*****—**Due to the randomness and uncertainty of wind energy, modern power systems integrating large-scale wind generation will be significantly impacted in terms of system performance and technical challenges. System inertia with high wind penetration is decreasing when conventional thermal generators are gradually replaced by wind turbines, which do not naturally contribute to inertia response. The power imbalance caused by wind power or demand fluctuations leads to the instability of system frequency. Accordingly, the need to attach the supplementary virtual inertia control to wind farms (WFs) strongly arises. When multi-wind farms are connected to the grid simultaneously, the selection of which critical WFs to install the virtual inertia control is greatly important to enhance the stability of system frequency. By building the small signal model of wind power systems considering frequency regulation, the installation locations are identified by the geometric measures of the mode observability of WFs. In addition, this paper takes the impacts of grid topology and selection of feedback control signals into consideration. Finally, simulations are conducted on a multi-wind farms power system and the results demonstrate that the designed virtual inertia control method can effectively assist the frequency regulation.

***Keywords*****—**Frequency regulation, virtual inertia control, installation locations, observability, wind farms.

## I. Introduction

POWER system with integrating significant amounts of wind generation is confronting with a series of challenges. The power imbalance will be caused by wind power fluctuation, which may result in some frequency stability issues [1]-[3]. As WFs are connected to the grid through the power electronic interfaces, the relation of the rotation speed and grid frequency is decoupled. Wind turbines with lower inertia cannot respond to the change of system frequency [2]. With increasing penetration of wind energy, the participation of wind turbines in frequency regulation have become an inevitable demand for enabling power system safe and stable operation. In recent years, more and more regions have raised relevant requirements for the participation of frequency regulation from wind turbines in different degrees [3].

The participation of wind turbines in frequency regulation can be implemented as follows: wind turbines operate in sub MPPT mode with power reserve [4]-[6], and the stored kinetic energy is released by using the supplementary control. The sub MPPT operation mode can be achieved by modifying the pitch or speed control system, which reduces the utilization of wind energy. The supplementary control strategies include the followings: 1) virtual inertia control with the derivation and deviation of frequency [7]-[9]; 2) virtual inertia control with super capacitor [10]; 3) virtual inertia control based on optimal power tracking [11]; 4) virtual synchronous control method [12]; 5) coordination with units, such as energy storage devices and FACTS [13].

For the sake of the supplementary control of WFs, the existing control methods for frequency regulation have not taken the dynamic distributed characteristics of grid frequency into consideration. When the power system operates in transient process, frequency responses at different buses are different from each other. In a real power system, the frequencies at different locations are measured via frequency measurement devices, such as Phasor Measurement Units (PMUs) and Frequency Disturbance Recorders (FDRs) [14]. In U. S power systems, Frequency Monitoring Network (FNET) was proposed to monitor the changes of system frequency all over the U. S, which can be used to identify a disturbance event within a power grid. Based on the frequency dynamic characteristics of the power system, this paper does further research on the frequency support provided by WFs.

The proposed model in [16] for frequency regulation cannot be applied to a power system with an infinite bus. When a power system contains an equivalent infinite bus, the frequency deviation will converge to zero in the steady state. As a result, the model does not take the dynamic distributed characteristics of system frequency into account. The presented method cannot assess the impact of the installation locations of WFs on system frequency. Hence, it is necessary to develop an effective method that suitable for the evaluation of a power system model with multi WF inputs and multi bus frequency outputs.

Most papers paid more attention on the frequency regulation and the optimal selection of the inertia control coefficients [3]-[10]. When multi-wind farms are connected to the main grid simultaneously, however, there are hardly any papers focus on the selection of WFs to add virtual inertia control to assist the power system frequency regulation. If multi-wind farms are connected to the power system, recommendations can be made for the selection of critical WFs to install virtual inertia controllers. By establishing the

W. Du is with the State Key Laboratory of Alternate Electric Power Systems with New Energy Resources, North China Electric Power University, Changping, Beijing, China (Corresponding author, e-mail: duwenjuanncepu@qq.com).

X. Wang, Jun Cao, and H. F. Wang are with the State Key Laboratory of Alternate Electric Power Systems with New Energy Resources, North China Electric Power University, Changping, Beijing, China.

small signal model of wind power systems with considering frequency regulation, the distributed characteristics of bus frequency can be evaluated. According to the observability of the bus frequency, critical WFs are then selected to add the virtual inertia controller to assist the power system frequency regulation. The system used for case study is the modified WSCC 3-machine 9-bus system with an infinite bus.

## II. Dynamic Frequency Characteristics

### A. Bus Frequency Measurement

Fig. 1 shows a schematic diagram of a general power system consisting of synchronous generators (SG), wind generators (WG) and loads.

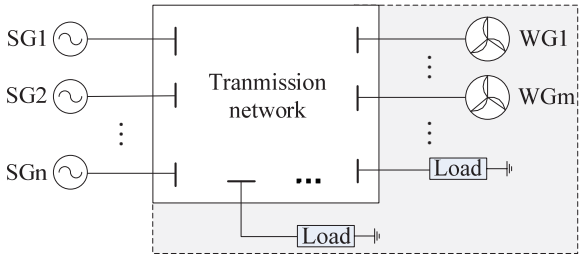


Fig. 1 Schematic diagram of a general power system

Based on the superposition theorem, the *i*th bus voltage can be written as:

$$U_i(t)=\sum_{j=1}^{ng}U_{i,j}(t)=\sum_{j=1}^{ng}U_{i,j}\cos(2\pi f_j+\theta_{i,j}) \quad (1)$$

where $U_{i,j}(t)$ is the *i*th bus voltage due to *j*th SG, $f_j$ is the frequency of *j*th SG. Note that *i*th bus voltage $U_i(t)$ is composed of multi-frequency voltages [15]. In steady state operation, a power system has a unified frequency $f_0$=50 Hz. The equivalent admittance matrix of the power system includes the original admittance matrix, WGs, loads and the internal impedances of SGs. The components corresponding to WGs and loads are expressed by using the equivalent injected current. For simplification, $U_i(t)$ can possess (?) its own bus frequency $f_i^{\text{mea}}$, then (1) can be rephrased by:

$$U_i^{\text{mea}}(t)=U_i^{\text{mea}}\cos(2\pi f_{\text{bus},i}^{\text{mea}}t+\theta_{i,j}^{\text{mea}}) \quad (2)$$

where $\theta_i^{\text{mea}}$ represents the phase angle of *i*th bus voltage. Equation (3) is obtained by using (1) and (2):

$$U_i^{\text{mea}}\cos(2\pi f_{\text{bus},i}^{\text{mea}}t+\theta_i^{\text{mea}})=\sum_{j=1}^{ng}U_{i,j}\cos(2\pi f_j+\theta_{i,j}) \quad (3)$$

Therefore, the estimated dynamic frequency at *i*th bus can be expressed as:

$$f_{\text{bus},i}^{\text{mea}}=\sum_{j}^{ng}\frac{U_{i,j}\cos(\theta_i^{\text{mea}}-\theta_{i,\text{j}})}{U_i^{\text{mea}}}f_j=\sum_{j}^{ng}C_{\text{f},j}f_j \quad (4)$$

### B. Two-Machine System

In order to investigate the dynamic distributed characteristics of bus frequencies, a two-machine system will be examined, as shown in Fig. 2. The parameters of synchronous machines SG1 and SG2 are identical and bus 1-5 are frequency monitoring points along with transmission line. $H_1$ and $H_2$ are the inertia constants of the SG1 and SG2 respectively.

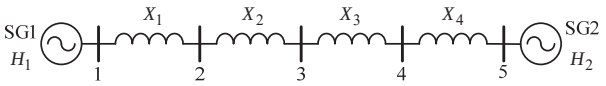


Fig. 2 Two-machine system

According to [16], the internal voltage angles can be expressed as: $\delta_1(t)=\delta_{1q}+k\sin(\omega_n t)$, $\delta_2(t)=\delta_{2q}-k\sin(\omega_n t)$, $\delta_{1q}$ and $\delta_{2q}$ are the steady-state values of $\delta_1$ and $\delta_2$, and $\omega_n$ is the system natural frequency.

The voltage angle along with transmission line can be written as:

$$\delta(z,t)=[\delta_{1q}-\delta_{2q}+2k\sin(\omega_n t)]\frac{l-z}{l}+\delta_{2q}-k\sin(\omega_n t) \quad (5)$$

where *l* is the total length of the transmission line, containing $X_{11}$ and $X_{22}$ which (represent) the distances from bus 1 and 5 to internal bus of SG1 and SG2, respectively. z is the distance from the internal bus of SG1 to bus 1. According to (5), the frequency at any point on the transmission line can be set as a function of *z*:

$$\Delta\omega(z,t)=\frac{\partial\delta(z,t)}{\partial t}=k\omega_n\cos(\omega_n t)[2\frac{l-z}{l}-1] \quad (6)$$

Note that the bus frequency deviation $\Delta\omega(z,t)$ will be zero when z=l/2. According to the concept of center of inertia, $\Delta\omega_c(t)=\frac{H_1\Delta\omega(z,t)\big|_{z=0}+H_1\Delta\omega(z,t)\big|_{z=l}}{H_1+H_2}$, bus 3 is the center of inertia.

If the frequency monitor equipment (FDR or PMU) is installed to the center-point, the frequency deviation cannot be observed. Based on (6), the farther the point from the center-point, the larger the frequency deviation will be. The system in Fig. 2 is used for simulation to verify the things mentioned above. As shown in Fig. 3, the frequencies measured at each bus are presented. Therefore, the simulation results are in accordance with the theoretical derivation conclusion.

### B. Distributed Characteristics of Bus Frequency

When performing a small-signal analysis, the linearized model of a power system can be given in a state space as:

$$\begin{cases} \Delta\dot{\mathbf{x}} = \mathbf{A}\Delta\mathbf{x} + \mathbf{B}\Delta\mathbf{u} \\ \Delta\mathbf{y} = \mathbf{C}\Delta\mathbf{x} + \mathbf{D}\Delta\mathbf{u} \end{cases} \quad (7)$$

where **A** is the system state matrix, **B** is the input matrix, and **C** is the output matrix, **D** is the feedforward matrix, **x** is the state vector, **u** is the control vector, and **y** is the output vector.

In order to characterize the relationship of bus frequencies, the geometric measures of observability (8), associated with the *i*th frequency mode is used.

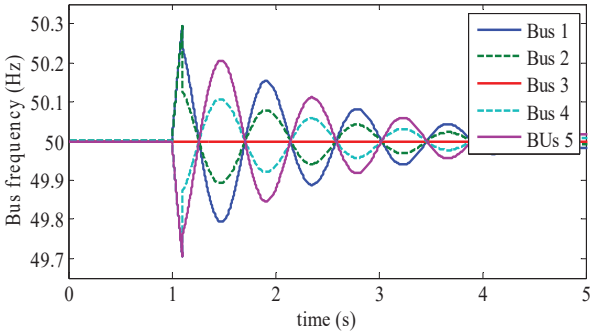


Fig. 3 Bus frequencies

$$gm_{oj}(i) = \cos(\theta(\mathrm{c}_j, f_i)) = \frac{|c_j f_i|}{\|f_i\|\|c_j\|} \quad (8)$$

where $c_j$ is the *j*th row of **C**, corresponding to bus *j*; $f_i$ is the *i*th right eigenvector of **A**; $\theta(\mathrm{c}_j, f_i)$ is the geometrical angle between the *j*th vector and the *i*th right eigenvector; $|\bullet|$ and $\|\bullet\|$ denote the modulus and Euclidean norm, respectively.

Fig. 4 shows the observabilities $gm_{oj}$ of bus frequencies. To simplify analysis, $gm_{oj}$ s are normalized which means the largest value is equal to 1. Thus, the $gm_{oj}$ index can indicate the difference among bus frequencies, and then be used to choose the feedback signal of frequency controller.

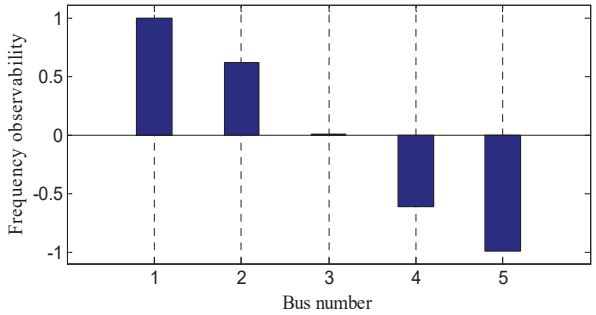


Fig. 4 Observabilities of bus frequencies

When machine 2 is replaced by an infinite bus, the bus frequencies and their observabilities are shown in Figs. 5 and 6 respectively, respectively. It is quite obvious that the simulation results are same as the previous two-machine system.

## III. Frequency Regulation by Using Virtual Inertia Control

In order to enable WFs to participate in frequency regulation, virtual inertia control signal is attached to the local real power controller by using a first order filter and a wash out filter. The signal is given as:

$$\Delta P^*_{Wref} = -K_{pf}\Delta f_{bus} - K_{df}\frac{d\Delta f_{bus}}{dt} \quad (9)$$

where $K_{pf}$ is the droop control coefficient, $K_{df}$ is the inertia control coefficient and $\Delta f_{bus}$ is the bus frequency deviation from the reference value $f_0$. The control scheme is presented in Fig. 7.

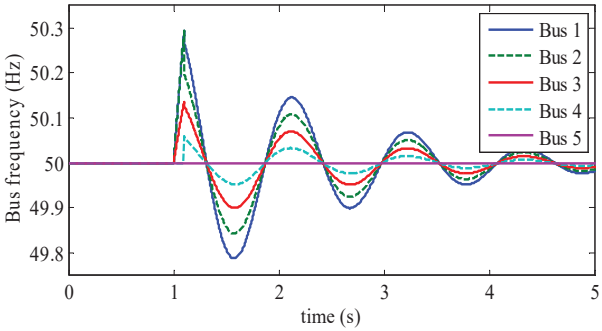


Fig. 5 Bus frequencies

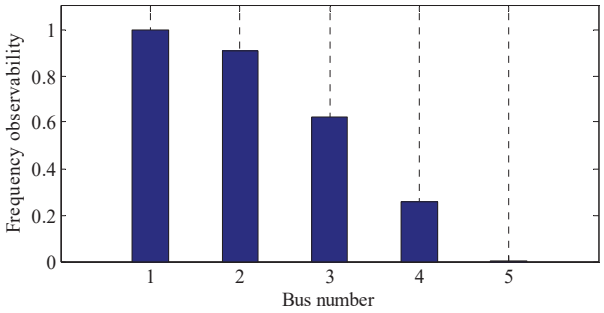


Fig. 6 Observabilities of bus frequencies

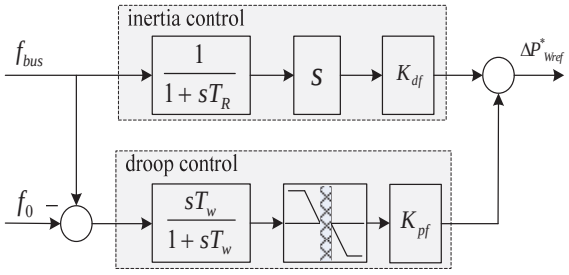


Fig. 7 Virtual inertial controller

Inertia control can provide frequency support by applying the derivative of the bus frequency to modify the power reference output. The stored kinetic energy supplied by inertial response is released by slowing the speed of wind turbine. The droop control can be utilized for WFs with power reserve margin to regulate system frequency primarily. Here we focus particularly on inertial control loop.

## IV. Simulation Study

Time domain simulation results are presented to verify the situations discussed in the previous sections. The power system shown in Fig. 8 [17] is used for this study, which consists of two generators, two DFIG-based WFs, three aggregated static loads, and one infinite bus. The detailed modelling of the DFIG is discussed in [9]. The power base is set to be 100 MVA. All the generators are conventional synchronous machines represented by the sub transient models and equipped with both excitation systems and governors.

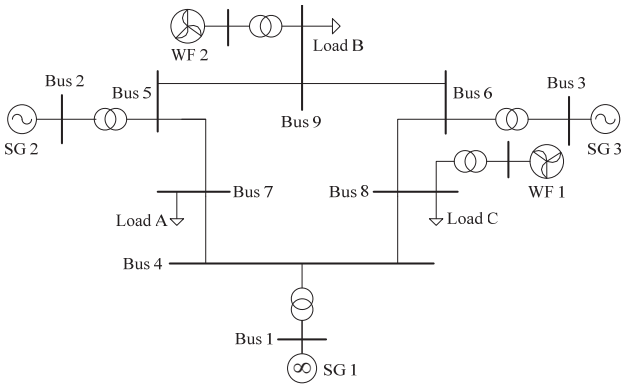


Fig. 8 WSCC 3-machine 9-bus system with WFs

The observabilities of the bus frequencies are shown in Fig. 9. The result shows that the observabilities of bus 1, 2 and 3 are smaller compared with those of bus 4, 5 and 6. Therefore WF2 which is connected to bus 9 is selected to install the virtual inertia controller.

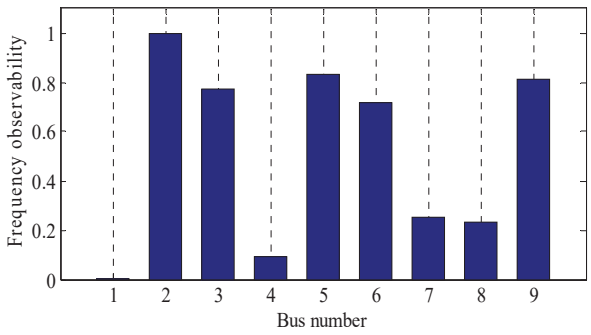


Fig. 9 Observability of bus frequency

### A. Frequency Regulation against Sudden Load Change

Fig. 10 (a) shows the bus frequency variations following a step increase in load at bus 5. As shown in Fig. 10 (b), frequency overshoot and settling time are significantly enhanced when WFs are participating in frequency regulation. More importantly, the frequency behaviour when both WF1 and WF2 are installed with inertia controller is almost same to the case when only WF1 is installed with the virtual inertia controller. In Figs. 10 (c) and (d), the transient performances (real power and rotor speed) are presented. When no virtual inertia control is added to WFs, the real power and the rotor speed of wind turbines are not practically affected. On the other hand, when both WF1 and WF2 are installed with virtual inertia control, the rotor speed decelerates, resulting in an increase in real power output. From Fig. 10 (c) it can be seen that real power injected by WF1 is significantly larger than WF1.

### B. Frequency Regulation against Generator Tripping

Fig. 11 (a) shows the bus frequency variations following the loss of the generator located at bus 2. The sizes of the bus frequencies are in accordance with their observabilities. As shown in Fig. 11 (b), it is also observed that the result verifies the previous analyses in Section IV-*A* and demonstrates that when virtual inertia controllers are installed in WF1 and WF2, the frequency behavior is similar to the result when only WF1 uses inertial control. Fig. 11 (c) also shows that the real power output of WF1 is larger than WF1 when the virtual inertia control is implemented in both WF1 and WF2. WF rotor speed is presented in Fig. 11 (d).

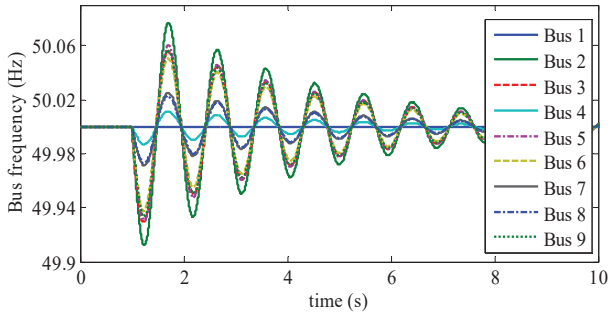


(a)

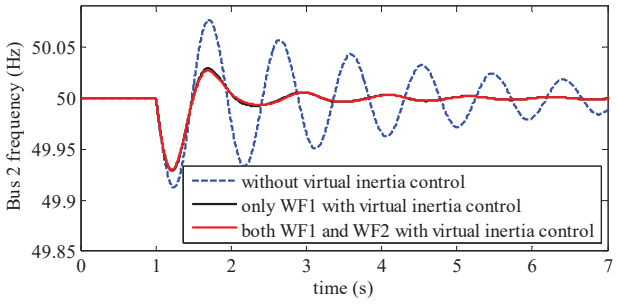


(b)

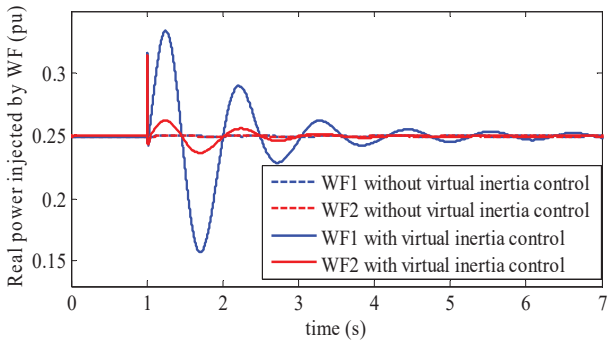


(c)

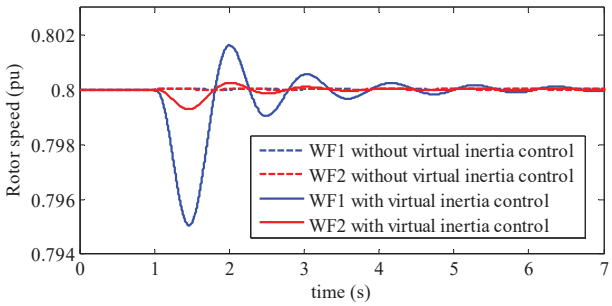


(d)

Fig. 10 Dynamic responses of system variables to sudden load change. (a) bus frequency without virtual inertia control, (b) frequency response at bus 2, (c) real power injected by WFs with virtual inertia control, (d) WF rotor speed

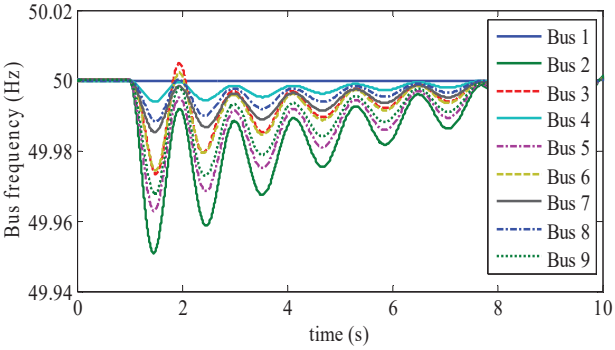


(a)

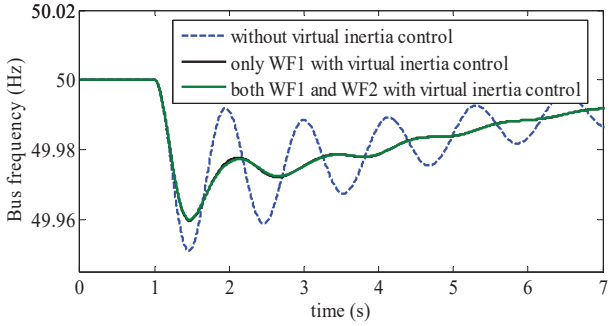


(b)

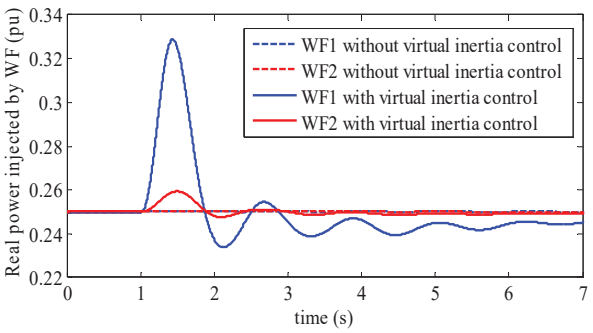


(c)

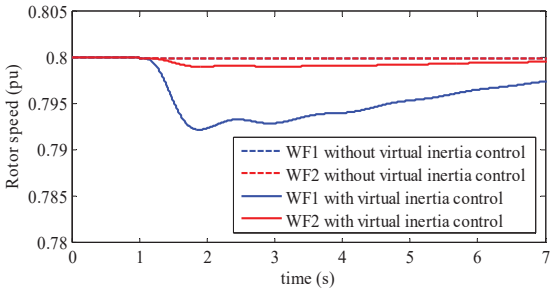


(d)

Fig. 11 Dynamic responses of system variables to generator tripping. (a) bus frequency without virtual inertia control, (b) frequency response at bus 2, (c) real power injected by WFs with virtual inertia control, (d) WF rotor speed

## V. Conclusion

This paper presents a method for selecting critical WFs to add virtual inertia control to assist the power system frequency regulation. A frequency measurement method is introduced to analyze the dynamic characteristics of bus frequency. Based on the established small signal model of wind power systems with taking frequency regulation into consideration, the critical WFs are selected to install the virtual inertia controllers. By using the proposed method, PMUs or FDRs can be installed at the critical WFs to monitor dynamic frequencies. A case study has been presented to demonstrate that the frequency regulation effectiveness by using selected WFs is equal to that using of overall WFs.

## Acknowledgment

This work is supported by the Fundamental Research Funds for the Central Universities (JB2015023) via the North China Electric Power University, Beijing, China, the National Basic Research Program of China (973Program) (2012CB215204), the NSFC project (51407068), China.

## References

[1] M. Tsili, S. Papathanassiou. "A review of grid code technical requirements for wind farms", *IET Renew. Power Generation*, vol. 3, pp. 308–332, Sept. 2009.

[2] J. Morren, J. Pierik, S. W. H. de Haan. "Inertial response of variable speed wind turbines", *Elect. Power Syst. Res.*, vol. 76, pp. 980–987, Jul. 2006.
[3] G. Ramtharan, J. B. Ekanayake, N. Jenkins. "Frequency support from doubly fed induction generator wind turbines", *IET Renew. Power Gen.*, vol. 1, pp. 3–9, Mar. 2007.
[4] R. G. de Almeida, E. D. Castronuovo, J. A. Peas Lopes. "Optimum generation control in wind parks when carrying out system operator requests", *IEEE Trans. Power Syst.*, vol. 21, pp. 718–725, May. 2006.
[5] N. R. Ullah, T. Thiringer, D. Karlsson. "Temporary primary frequency control support by variable speed wind turbines—potential and applications", *IEEE Trans. Power Syst.*, vol. 23, pp. 601–612, May. 2008.
[6] K. V. Vidyanandan, N. Senroy. "Primary frequency regulation by deloaded wind turbines using variable droop", *IEEE Trans. Power Syst.*, vol. 28, pp. 837–846, May. 2013.
[7] J. Ekanayake, N. Jenkins. "Comparison of the response of doubly fed and fixed-speed induction generator wind turbines to changes in network frequency", *IEEE Trans. Energy Convers.*, vol. 19, pp. 800–802, Dec. 2004.
[8] J. Morren, S.W.H. de Haan, W. L. Kling, J. A. Ferreira. "Wind turbines emulating inertia and supporting primary frequency control", *IEEE Trans. Power Syst.*, vol. 21, pp. 433–434, Feb. 2006.
[9] D. Margaris, S. A. Papathanassiou, N. D. Hatziargyriou, A. D. Hansen, P. Sørensen. "Frequency control in autonomous power systems with high wind power penetration". *IEEE Trans. Power Syst.*, vol. 3, pp. 189–199, Apr. 2012.
[10] M. F. M. Arani, E. F. El-Saadany. "Implementing virtual inertia in DFIG-based wind power generation", *IEEE Trans. Power Syst*., vol. 28, pp.1373–1384, May. 2013.
[11] Z. Zhang, Y. Wang, H. Li, Z. Su. "Comparison of inertia control methods for DFIG-based wind turbines", *Proc. IEEE ECCE Asia Downunder (ECCE Asia)*, Jun. 2013, pp. 960–964.
[12] S. Wang, J. Hu, X. Yuan. "Virtual synchronous control for grid-connected DFIG-based wind turbines", *IEEE Journal of Emerging and Selected Topics in Power Electronics*, to be published.
[13] D. Banham-Hall，G. Taylor, C. Smith, M. Irving. "Flow batteries for enhancing wind power integration", *IEEE Trans. On Power Systems*, vol. 27, pp. 1690-1697, Aug. 2012.
[14] Y. Zhang, et al. "Wide-area frequency monitoring network (FNET) architecture and applications", *IEEE Trans. Smart Grid*, vol. 1, pp. 159–168, Sept. 2010.
[15] M. A. Tabrizi. "Participation of non-conventional energy resources in power system frequency control", *Ph.D. dissertation*, Tennessee Technological University, 2013.
[16] M. W. Baldwin, Y. Liu, F. M. Nurogru. "Generator outage identification by use of electromechanical state-space modal analysis", *IEEE Trans. Power Syst*., Vol.29, pp.1831-1838, Jul. 2014.
[17] P. W. Sauer and M. A. Pai. *Power System Dynamics and Stability*. Hong Kong: Pearson Education Asia, First Indian Reprint, 2002.